ADVANCED FUNCTIONAL MATERIALS

Supporting Information

for *Adv. Funct. Mater.,* DOI: 10.1002/adfm.202003660

The Role of Ni and Co in Suppressing O-Loss in Li-Rich Layered Cathodes

*Edouard Boivin, Niccolo Guerrini, Robert A. House, Juan G. Lozano, Liyu Jin, Gregory J. Rees, James W. Somerville, Christian Kuss, Matthew R. Roberts, and Peter G. Bruce**

Supplementary information:

The role of Ni and Co in suppressing O-loss in Li rich layered cathodes

Edouard Boivin[1, Δ], Niccolo Guerrini[1], Robert A. House[1], Juan G. Lozano[1], Liyu Jin[1], Gregory J. Rees[1], James W. Somerville[1], Christian Kuss[1], Matthew R. Roberts[1] and Peter G. Bruce[1,*].

1. Departments of Materials and Chemistry, University of Oxford, Parks Road, OX3 1PH, U.K.

* Corresponding author: peter.bruce@materials.ox.ac.uk

Δ Curent affiliation: Univ. Lille, CNRS, Centrale Lille, ENSCL, UMR 8181-UCCS Unité de Catalyse et Chimie du Solide, F-59000 Lille, France

Table S1: chemical composition (ICP), specific surface (BET), density (pycnometry) and average primary particle size (obtained from the BET surface and the pycnometric density and assuming spherical particles, with $d_{average} = 6/ (S_{BET} \cdot \rho_{pycnometry})$) for all the materials studied in this article. All compounds show similar particle size (~ 110 nm), BET surface (~ 13 m^2/g) and elemental ICP ratios in good agreement with the targeted compositions.

	ICP				BET Surface (m^2/g)	Pycnometry density (g/cm^3)	Average Approximated particle size (nm)
	Li	Ni	Mn	Co			
$Li_{1.29}Ni_{0.06}Mn_{0.65}O_2$	1.28(1)	0.07(1)	0.65	0	13.80(3)	3.94(1)	110(1)
$Li_{1.25}Ni_{0.12}Mn_{0.63}O_2$	1.26(1)	0.11(1)	0.63	0	12.75(4)	4.02(1)	117(1)
$Li_{1.2}Ni_{0.2}Mn_{0.6}O_2$	1.20(1)	0.20(1)	0.60	0	13.06(2)	4.11(1)	112(1)
$Li_{1.13}Ni_{0.3}Mn_{0.56}O_2$	1.12(1)	0.31(1)	0.56	0	13.77(5)	4.22(1)	103(1)
$Li_{1.07}Ni_{0.4}Mn_{0.53}O_2$	1.09(1)	0.38(1)	0.53	0	13.20(2)	4.02(2)	113(1)
$Li_{1.2}Ni_{0.13}Co_{0.13}Mn_{0.54}O_2$	1.19(1)	0.14(1)	0.54	0.13(1)	13.46(4)	4.36(1)	102(1)
$Li_{1.31}Co_{0.06}Mn_{0.63}O_2$	1.30(1)	0	0.63	0.07(1)	12.56(6)	3.80(1)	125(1)
$Li_{1.29}Co_{0.12}Mn_{0.59}O_2$	1.27(1)	0	0.59	0.14(1)	11.83(3)	4.00(1)	126(1)
$Li_{1.27}Co_{0.20}Mn_{0.53}O_2$	1.25(1)	0	0.53	0.22(1)	12.89(4)	4.21(2)	110(1)
$Li_{1.23}Co_{0.30}Mn_{0.47}O_2$	1.22(1)	0	0.47	0.31(1)	12.95(2)	4.27(1)	108(1)
$Li_{1.20}Co_{0.40}Mn_{0.40}O_2$	1.21(1)	0	0.40	0.39(1)	12.14(3)	4.35(2)	113(1)
$Li_{1.10}Co_{0.70}Mn_{0.20}O_2$	1.12(1)	0	0.20	0.68(1)	10.92(3)	4.78(1)	114(1)

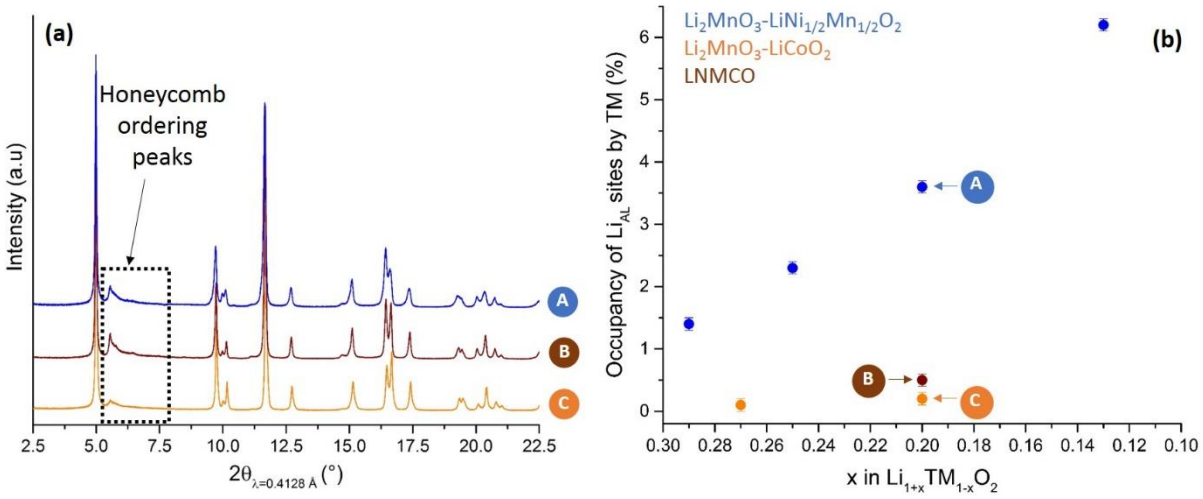

Figure S1: *(a) Synchrotron XRD pattern of LNMO (blue), LNMCO (brown) and LMCO (orange). The superstructure peaks indicate the presence of the honeycomb ordering. (b) Evolution of the TM/Li anti-site defects between the transition metal and alkali metal layers as a function of the Li-richness for the materials belonging to the Li_2MnO_3-$LiCoO_2$ (orange), Li_2MnO_3-$LiNi_{1/2}Mn_{1/2}O_2$ (blue) and for LNMCO (brown). TM/Li anti-site defects are more abundant along the Li_2MnO_3-$LiNi_{1/2}Mn_{1/2}O_2$ tie-line compared to the Co containing materials.*

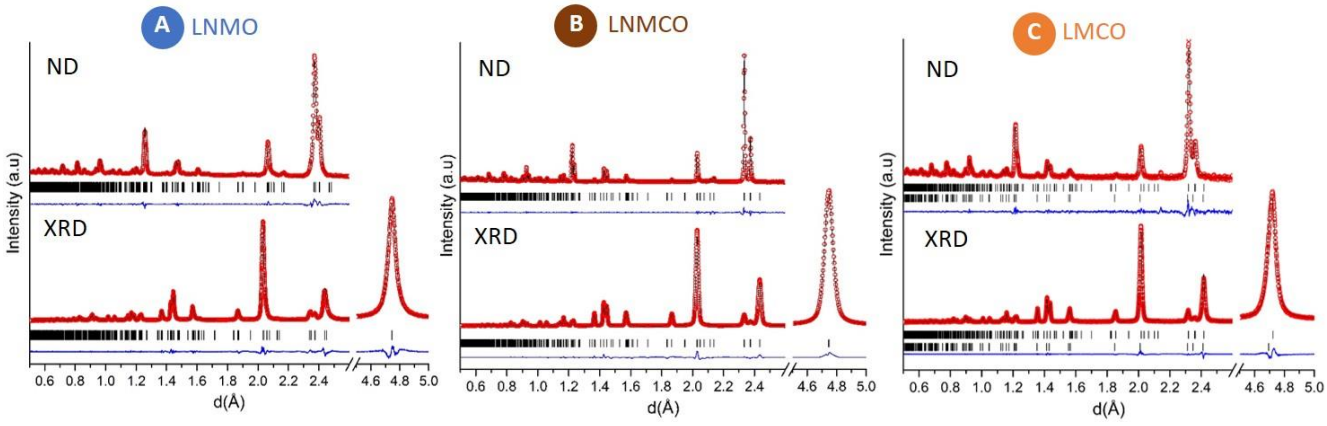

Figure S2: Joint Rietveld refinements of the structures of (a) LNMO, (b) LMCO and (c) LNMCO based on synchrotron XRD and ND data using the C2/m space group. The details of the refinement procedure are given below.

Joint XRD and ND Rietveld refinements have been performed using the C2/m space group (which captures the honeycomb ordering in the transition metal layers) and keeping the global composition as constant. For LMCO, $LiCoO_2$ has been included as an additional phase as it is known to be present at this composition, see for example the NMR data in Fig. S5. The concentration of Li/TM anti-site defects between the transition metal and alkali metal layers and the nature of the cations involved (Ni, Co, or Mn) has been refined. However, for LNMCO we've assumed the presence of Li/(Ni, Co) rather than Li/(Ni, Co, Mn) anti-site defects, as it isn't possible to refine partial occupancies of these 4 elements in a single Wyckoff position. The in-plane anti-site defects (*i.e.* Mn in Li_{TML} site of the Li_2MnO_3 structure) has also been investigated but it was found in all cases that this kind of cation mixing is negligible.

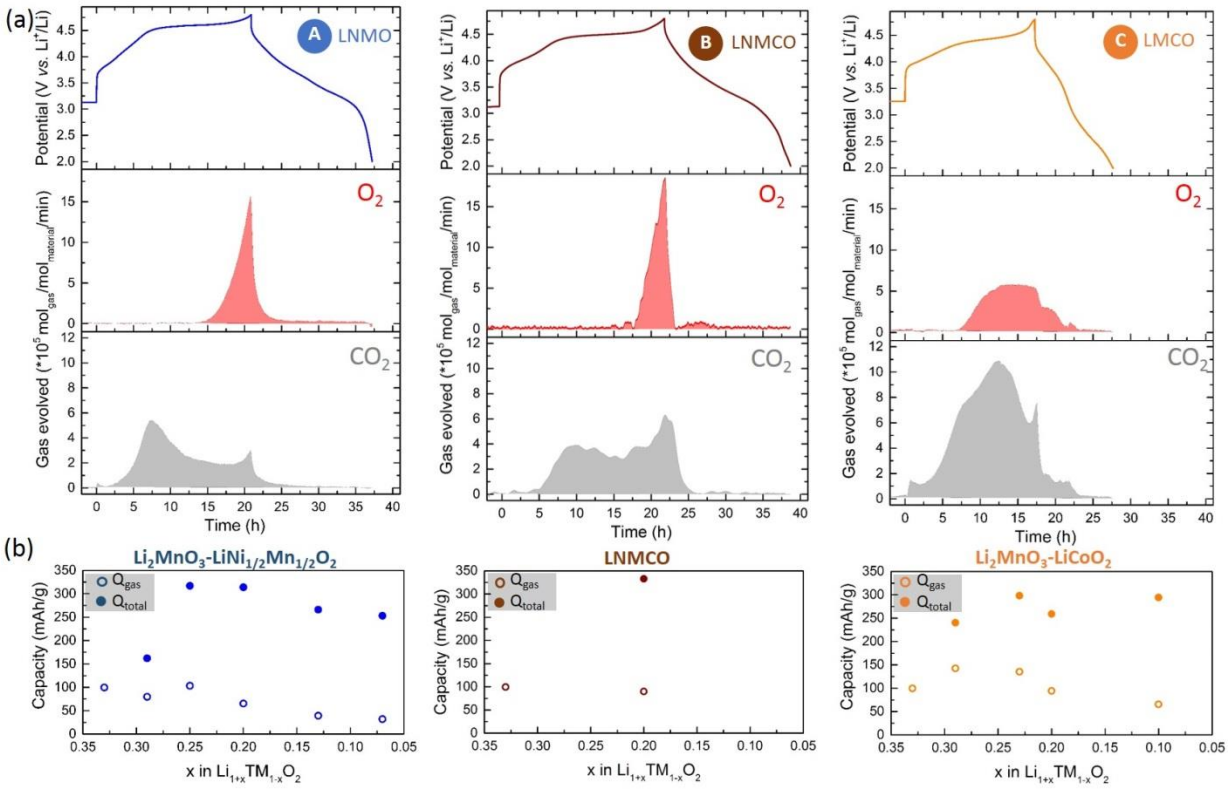

Figure S3: (a) OEMS analysis LNMO, LNMCO and LMCO. In the panels are shown the galvanostatic curve during the first cycle, the O_2 (red) and the CO_2 (grey) traces ($mol_{gas}/mol_{material}/min$). The CO_2 evolution observed before the end of the TM redox region on charge (i.e. before the beginning of the plateau) is consistent with the incomplete oxidation of Ni^{2+} in the shell – as seen in all Ni containing Li layered oxides[1,2]-

which is charge compensated by O-redox near the surface of particles and hence O-release. (b) Capacities associated with O loss determined from the OEMS, circles, and the total capacities, dots, for Li_2MnO_3-$LiNi_{1/2}Mn_{1/2}O_2$ (blue), Li_2MnO_3-$LiCoO_2$ (orange) tie-lines and for LNMCO (brown). The capacities calculated for the gas evolution are based on the equation provided in the experimental section. It shows that decreasing the Li-richness and/or increasing Ni content suppress O-loss.

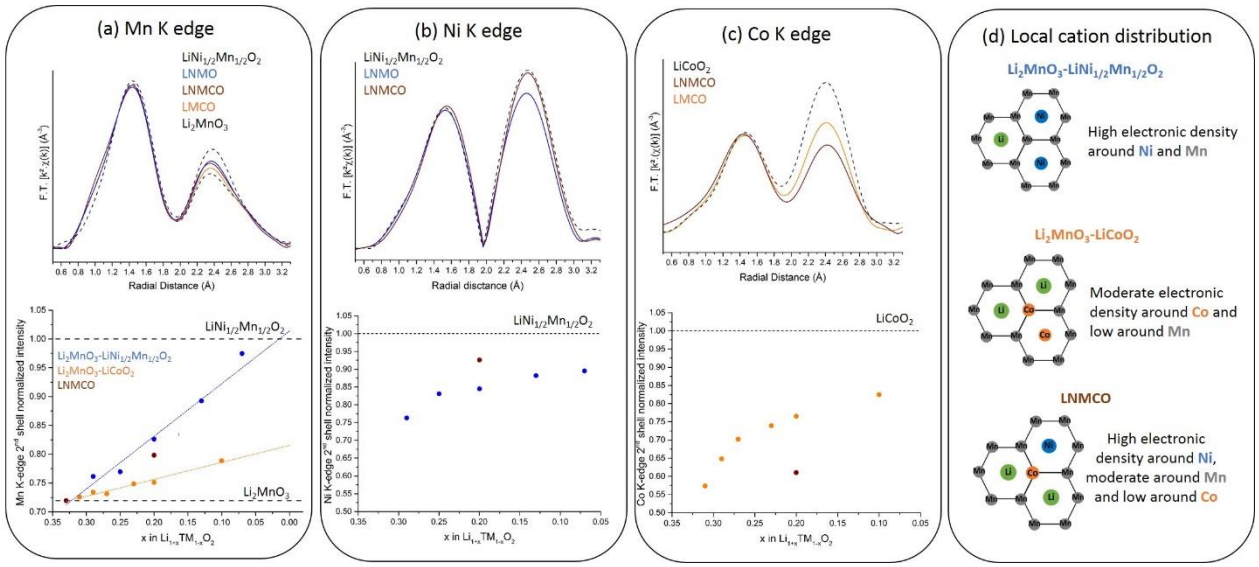

Figure S4: (a) Mn, (b) Ni and (c) Co K-edge EXAFS spectra of LNMO, LNMCO, LMCO, $LiNi_{1/2}Mn_{1/2}O_2$, $LiCoO_2$ and Li_2MnO_3 (top panels) and the corresponding evolution of $2^{nd}/1^{st}$ shell EXAFS intensity ratio as a function of the Li-richness for all materials synthetized in this study (bottom panels). (d) The schematic representation of the local cation distribution within the TM layer in the bulk of the materials explaining the intensity ratios observed at each edge and along each tie-line.

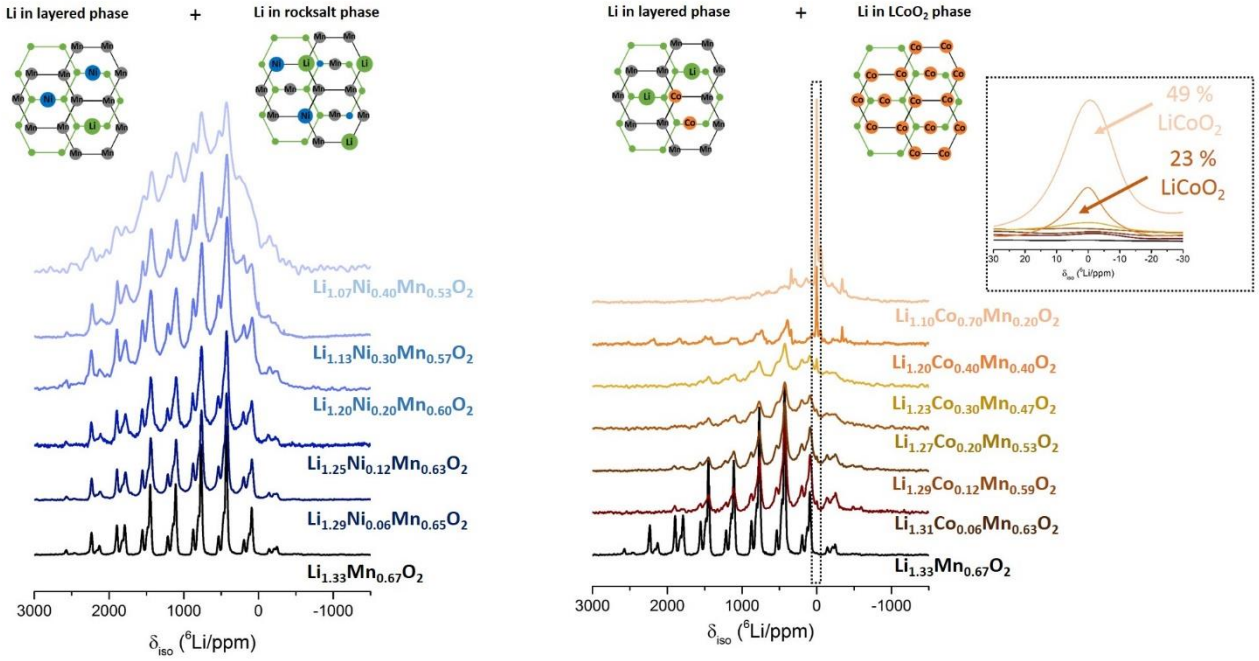

Figure S5: ^{6}Li MAS NMR data collected for all compositions along the Li_2MnO_3-$LiNi_{0.5}Mn_{0.5}O_2$ (a) and the Li_2MnO_3-$LiCoO_2$ (b) tie-lines. A schematic representations of the local cation distribution explaining the different NMR contributions observed are also represented. A Li_2MnO_3-like component is observed in all spectra. In addition along the Li_2MnO_3-$LiNi_{0.5}Mn_{0.5}O_2$ tie-line a disordered contribution grows with Ni content while along Li_2MnO_3-$LiCoO_2$ tie-line a $LiCoO_2$ peak grows from $Li_{1.27}Co_{0.2}Mn_{0.53}O_2$ (see enlargement of the diamagnetic contribution shown in inset).

References

[1] W.-S. Yoon, M. Balasubramanian, K. Y. Chung, X.-Q. Yang, J. McBreen, C. P. Grey, D. A. Fischer, *J. Am. Chem. Soc.* **2005**, *127*, 17479.

[2] W.-S. Yoon, M. Balasubramanian, X.-Q. Yang, Z. Fu, D. A. Fischer, J. McBreen, *J. Electrochem. Soc.* **2004**, *151*, A246.